Faster Resolution of the 3-D Forward Problems in Microwave Imaging by a Partial-Block BiCGStab Algorithm

Corentin Friedrich[1,2], Sébastien Bourguignon[1], Jérôme Idier[1], Yves Goussard[2]
[1]LUNAM Université, École Centrale de Nantes / IRCCyN UMR CNRS 6597, 1 rue de la Noë, 44321 Nantes, France
[2]École Polytechnique de Montréal, Dept. of Electrical Engineering, C.P. 6079, H3C 3A7, Montréal QC, Canada

***Abstract*—In microwave image reconstruction, the biconjugate gradient stabilized (BiCGStab) algorithm is generally used to solve the 3-D forward problem. In practice, the number of forward problems that must be solved simultaneously is equal to the number of available illuminations. Here, we propose the use of a block version of the BiCGStab algorithm that can take advantage of the fact that all forward problems share the same linear operator, thereby significantly reducing the amount of computation. In order to make the technique faster and more robust, an implementation based on a partition of the illuminations into subsets is introduced. Simulations are carried out on a realistic setup for image reconstruction and reveal the superiority of the proposed algorithm over the BiCGStab method, mainly for high contrasted objects.**

***Index Terms*—Electromagnetics, 3-D microwave imaging, forward problem, inverse problem, biconjugate gradient stabilized method.**

I. Introduction

Microwave imaging techniques have undergone considerable development in the past few years, and applications in areas like biomedical imaging and nondestructive testing appear promising. [1], [2]. However, these techniques present methodological difficulties (ill-posedness, presence of nonlinearities) which make solutions computationally expensive, particularly for three-dimensional problems. Indeed, reducing the computational cost of the reconstruction methods is a crucial challenge.

Many full-wave 3-D reconstruction algorithms are based on the minimization of a regularized least-squares objective function. Minimization is generally carried out using gradient-based optimization procedures [2], [3]. At each iteration, determining a descent direction and performing the line search require the resolution of 3-D forward problems, *i.e.,* the determination of the total electric fields everywhere in the 3-D domain of interest. Solving a forward problem amounts to inverting a linear system. In practical situations, computational and memory limitations make it impossible to compute the exact solution for real-size problems and one has to rely on approximate solutions produced by iterative techniques such as conjugate gradient [4], biconjugate gradient [5] or quasi minimal residual (QMR) approaches. Recently, the *biconjugate gradient stabilized* (BiCGStab) algorithm, developed in [6], has become the most popular choice [1]–[3].

In 3-D microwave imaging, the forward problem must be computed for several illuminations. However, one may take advantage of the fact that the matrix of the linear system is identical for all illuminations to reduce the computational cost. A first possibility is the parallelization of these operations on multiple processors to perform the resolutions simultaneously [2], [7]. A linear speedup parallelization factor is almost obtained. Another possibility is to rely on block versions of the aforementioned iterative algorithms [8]. The idea is to jointly solve multiple right-hand sides with a unique linear operator. A block-QMR method was proposed for microwave image reconstruction [9]. In [10], a block version of BiCGStab (Block-BiCGStab) was developed and was proved to outperform the block-QMR algorithm on generic problems.

In this paper, we propose the use of Block-BiCGStab for solving the 3-D forward problem with multiple sources in microwave imaging. For problems with a large number of sources, we introduce a Partial-Block BiCGStab version based on a specific partition of the illuminations in order to make the algorithm more robust. In Section II, the 3-D microwave forward problem is established using the integral formulation and a discretization by the method of moments. Then the Block-BiCGStab algorithm and the Partial-Block version are detailed in Section III. Simulation results are given in Section IV where the computational costs of the different versions of BiCGStab are compared.

II. 3-D forward problem formulation

The forward problem in microwave tomography consists of determining the total electric field in a domain V from the scattering of an incident wave by a known dielectric object included in V. Here, we assume that this object is nonmagnetic and is characterized by its complex permittivity $\epsilon(\boldsymbol{r})$, where $\boldsymbol{r}$ denotes the spatial position. This volume is immersed in a homogeneous background medium with complex permittivity ϵ_b and magnetic permeability μ_b. The object is successively illuminated by n_S known time-harmonic incident fields with angular frequency ω. In the sequel, the time dependence term $e^{-j\omega t}$ is omitted. The complex 3-D vector field $\boldsymbol{E}_i^{\text{inc}}(\boldsymbol{r})$

represents the amplitude and the phase of the three spatial components of the i-th incident electric field at the location $\boldsymbol{r}$.

The total field is defined by the sum of the incident field and the scattered field generated by the object. Using the integral equation formulation, the total field $\boldsymbol{E}_i(\boldsymbol{r})$ is given by the nonlinear domain integral equation [11]:

$$\boldsymbol{E}_i(\boldsymbol{r}) = \boldsymbol{E}_i^{\text{inc}}(\boldsymbol{r}) + \left(k_b^2 + \nabla\nabla\cdot\right) \int_V g(\boldsymbol{r},\boldsymbol{r}')\chi(\boldsymbol{r}')\boldsymbol{E}_i(\boldsymbol{r}')d\boldsymbol{r}', \quad \forall \boldsymbol{r} \in V. \quad (1)$$

where the wavenumber, the contrast function and the homogeneous Green function respectively read $k_b^2 = \omega^2\mu_b\epsilon_b$, $\chi(\boldsymbol{r}) = (\epsilon(\boldsymbol{r}) - \epsilon_b)/\epsilon_b$, and:

$$g(\boldsymbol{r},\boldsymbol{r}') = \frac{\exp\left(jk_b\|\boldsymbol{r}-\boldsymbol{r}'\|\right)}{4\pi\|\boldsymbol{r}-\boldsymbol{r}'\|}. \quad (2)$$

The $\nabla\nabla\cdot$ term corresponds to the gradient of the divergence. The second term of the right-hand side of (1) corresponds to the scattered field. Note that $g(\boldsymbol{r},\boldsymbol{r}')$ is a convolution kernel with a singularity at $\boldsymbol{r} = \boldsymbol{r}'$.

In practice, (1) is discretized and V is divided into n cubic cells. We assume that V is a cuboid with dimensions N_x, N_y and N_z, so that $n = N_xN_yN_z$. Let $\boldsymbol{e}_i^x$ (respectively $\boldsymbol{e}_i^y$ and $\boldsymbol{e}_i^z$) denote the vector of length n corresponding to the x- (respectively y- and z-) component of the total electric field discretized onto the n voxels. Similarly, we note $\boldsymbol{e}_i^{\text{inc}\,x}$, $\boldsymbol{e}_i^{\text{inc}\,y}$ and $\boldsymbol{e}_i^{\text{inc}\,z}$ the components of the incident field on the n voxels. Using the method of moments [12] and the weakening of the singularity of $g(\boldsymbol{r},\boldsymbol{r}')$ as in [13], the discretized version of (1) reads:

$$\begin{bmatrix}\boldsymbol{e}_i^x\\ \boldsymbol{e}_i^y\\ \boldsymbol{e}_i^z\end{bmatrix} = \begin{bmatrix}\boldsymbol{e}_i^{\text{inc}\,x}\\ \boldsymbol{e}_i^{\text{inc}\,y}\\ \boldsymbol{e}_i^{\text{inc}\,z}\end{bmatrix} + k_b^2 \begin{bmatrix}\mathbf{G}_1 & \mathbf{0}_{n,n} & \mathbf{0}_{n,n}\\ \mathbf{0}_{n,n} & \mathbf{G}_1 & \mathbf{0}_{n,n}\\ \mathbf{0}_{n,n} & \mathbf{0}_{n,n} & \mathbf{G}_1\end{bmatrix} \begin{bmatrix}\mathbf{X} & \mathbf{0}_{n,n} & \mathbf{0}_{n,n}\\ \mathbf{0}_{n,n} & \mathbf{X} & \mathbf{0}_{n,n}\\ \mathbf{0}_{n,n} & \mathbf{0}_{n,n} & \mathbf{X}\end{bmatrix} \begin{bmatrix}\boldsymbol{e}_i^x\\ \boldsymbol{e}_i^y\\ \boldsymbol{e}_i^z\end{bmatrix} + \mathbf{D} \begin{bmatrix}\mathbf{G}_2 & \mathbf{0}_{n_2,n} & \mathbf{0}_{n_2,n}\\ \mathbf{0}_{n_2,n} & \mathbf{G}_2 & \mathbf{0}_{n_2,n}\\ \mathbf{0}_{n_2,n} & \mathbf{0}_{n_2,n} & \mathbf{G}_2\end{bmatrix} \begin{bmatrix}\mathbf{X} & \mathbf{0}_{n,n} & \mathbf{0}_{n,n}\\ \mathbf{0}_{n,n} & \mathbf{X} & \mathbf{0}_{n,n}\\ \mathbf{0}_{n,n} & \mathbf{0}_{n,n} & \mathbf{X}\end{bmatrix} \begin{bmatrix}\boldsymbol{e}_i^x\\ \boldsymbol{e}_i^y\\ \boldsymbol{e}_i^z\end{bmatrix} \quad (3)$$

where $\mathbf{X}$ is an $n \times n$ diagonal matrix whose diagonal contains the discretized contrast samples. $\mathbf{G}_1$ is an $n \times n$ convolution matrix corresponding to the discretization of $g(\boldsymbol{r},\boldsymbol{r}')$ for all couples of voxels with centers $\boldsymbol{r}$ and $\boldsymbol{r}'$. The $3n\times3n_2$ matrix $\mathbf{D}$ corresponds to the finite-difference discretization of the $\nabla\nabla\cdot$ term, where $n_2 = (N_x+2)(N_y+2)(N_z+2)$. The $n_2\times n$ matrix $\mathbf{G}_2$ is similar to $\mathbf{G}_1$, as it corresponds to the discretization of $g(\boldsymbol{r},\boldsymbol{r}')$ on the cuboid defined by adding a one-voxel layer on each face of V. This is required because of the finite-difference form of the $\nabla\nabla\cdot$ term. Matrix $\mathbf{0}_{n,m}$ denotes the $n \times m$ null matrix.

For the sake of clarity, we rewrite (3) in compact matrix form:

$$\boldsymbol{e}_i = \boldsymbol{e}_i^{\text{inc}} + k_b^2\mathbf{G}_1^{(3)}\mathbf{X}^{(3)}\boldsymbol{e}_i + \mathbf{D}\mathbf{G}_2^{(3)}\mathbf{X}^{(3)}\boldsymbol{e}_i \quad (4)$$

where $\boldsymbol{e}_i$ and $\boldsymbol{e}_i^{\text{inc}}$ denote the vectors with length $3n$ containing the three components of the total and incident fields respectively. The superscript $^{(3)}$ means that the above matrices are block-diagonal with three blocks. (4) can be written as a standard linear system:

$$\boldsymbol{e}_i^{\text{inc}} = \mathbf{L}\boldsymbol{e}_i \quad (5)$$

$$\text{with} \quad \mathbf{L} = \mathbf{I}_{3n} - k_b^2\mathbf{G}_1^{(3)}\mathbf{X}^{(3)} - \mathbf{D}\mathbf{G}_2^{(3)}\mathbf{X}^{(3)} \quad (6)$$

where $\mathbf{I}_{3n}$ denotes the identity matrix of size $3n$.

Solving the forward problem for one illumination of incident field $\boldsymbol{e}_i^{\text{inc}}$ requires the resolution of (5) , which cannot be carried out exacly in large-scale problems. Iterative approaches, such as the BiCGStab algorithm [2], [3], are usually used to compute efficiently the forward problem. Such methods require a large number of multiplications with matrix $\mathbf{L}$ which are the most consuming operations. Even if $\mathbf{G}_1$ and $\mathbf{G}_2$ are convolution matrices and then the multiplications with $\mathbf{L}$ can be carried out using Fast Fourier Transform (FFT) routines, the computational cost of the multiplications still remains high.

III. Block Resolution of the forward problem

Microwave image reconstruction algorithms require the resolution of n_S forward problems of type (5) at each iteration of the minimization scheme. Since the operator $\mathbf{L}$ does not depend on the sources, the multiple linear systems can be gathered as:

$$\mathbf{E}^{\text{inc}} = \mathbf{L}\mathbf{E} \quad (7)$$

with $\mathbf{E}^{\text{inc}} = \left[\boldsymbol{e}_1^{\text{inc}}, \ldots, \boldsymbol{e}_{n_s}^{\text{inc}}\right]$ and $\mathbf{E} = [\boldsymbol{e}_1, \ldots, \boldsymbol{e}_{n_s}]$. This structure lends itself to resolution by block versions of iterative algorithms, such as the Block-BiCGStab method proposed hereafter.

For comparative purposes, the pseudo-code of the BiCGStab algorithm is given in Algorithm 1. The symbol † denotes the Hermitian adjoint. BiCGStab has to be called n_S times to solve (7), one for each incident field $\boldsymbol{e}_i^{\text{inc}}$. Multiplications with $\mathbf{L}$ occurs twice at each iteration (steps 5 and 8). These two steps are the most consuming operations. The residual error at iteration k is $\boldsymbol{r}_k = \boldsymbol{e}^{\text{inc}} - \mathbf{L}\boldsymbol{e}_k$. The Block-BiCGStab algorithm (the block version of BiCGStab) is defined in [10] and is detailed in Algorithm 2. The notation $\langle\mathbf{T},\mathbf{S}\rangle_F$ is the Frobenius product, *i.e.*, Trace$\left(\mathbf{T}^\dagger\mathbf{S}\right)$. Block-BiCGStab has to be called only once for all illuminations. At each iteration, n_S multiplications in step 5 and n_S multiplications in step 8 are performed. Matrix $\mathbf{R}_k$ represents the set of residuals for all illuminations. BiCGStab is stopped when $\boldsymbol{r}_k$ is smaller than a tolerance defined by the user. Block-BiCGStab is stopped when all residual errors, *i.e.*, all the columns of $\mathbf{R}_k$, are small enough. Let us remark that for $n_S = 1$, Block-BiCGStab is equivalent to BiCGStab.

Steps 6 and 12 in Algorithm 2 require the resolution of linear systems of size n_S. Due to their small size, these systems can be solved exactly. However, matrix $\widetilde{\mathbf{R}}_0^\dagger\mathbf{V}$ may become singular or ill-conditioned in the iterative process [10].

Algorithm 1 BiCGStab algorithm

Initialize $\boldsymbol{e}_0$, $\boldsymbol{r}_0 = \boldsymbol{e}^{\text{inc}} - \mathbf{L}\boldsymbol{e}_0$, $\boldsymbol{p}_0 = \boldsymbol{r}_0$
Choose an arbitrary $\tilde{\boldsymbol{r}}_0$
$k = 0$
while $\left(\|\boldsymbol{r}_k\|/\|\boldsymbol{e}^{\text{inc}}\| > \text{tolerance}\right)$ **do**
  $\boldsymbol{v} = \mathbf{L}\boldsymbol{p}_k$
  $\alpha = \tilde{\boldsymbol{r}}_0^\dagger \boldsymbol{r}_k / \tilde{\boldsymbol{r}}_0^\dagger \boldsymbol{v}$
  $\boldsymbol{s} = \boldsymbol{r}_k - \alpha \boldsymbol{v}$
  $\boldsymbol{t} = \mathbf{L}\boldsymbol{s}$
  $\omega = \boldsymbol{t}^\dagger \boldsymbol{s} / \boldsymbol{t}^\dagger \boldsymbol{t}$
  $\boldsymbol{e}_{k+1} = \boldsymbol{e}_k + \alpha \boldsymbol{p}_k + \omega \boldsymbol{s}$
  $\boldsymbol{r}_{k+1} = \boldsymbol{s} - \omega \boldsymbol{t}$
  $\beta = (\alpha \tilde{\boldsymbol{r}}_0^\dagger \boldsymbol{r}_{k+1}) / (\omega \tilde{\boldsymbol{r}}_0^\dagger \boldsymbol{r}_k)$
  $\boldsymbol{p}_{k+1} = \boldsymbol{r}_{k+1} + \beta(\boldsymbol{p}_k - \omega \boldsymbol{v})$
  $k \leftarrow k + 1$
end while

For instance, if two sources are very close, then the two corresponding columns of $\mathbf{E}^{\text{inc}}$ are highly correlated. The consequence is that $\mathbf{R}_0$ and $\mathbf{V}$ may be ill-conditioned, resulting in potential instabilities of Block-BiCGStab. In order to solve this issue, we propose a procedure called *Partial-Block BiCGStab* formulated in Algorithm 3. Rather than dealing with all illuminations simultaneously, the sources are divided into P subgroups. The partition is chosen such that the sources of each subgroup are weakly correlated with one another. The matrix of incident fields $\mathbf{E}^{\text{inc}}$ is then divided into P submatrices $\mathbf{E}^{\text{inc}^p}$ in which the columns are the least correlated. Then, Block-BiCGStab is applied on each group. Note that for $P = n_S$, the Partial-Block BiCGStab algorithm is equivalent to the BiCGStab method. For $P = 1$, it corresponds to the Block-BiCGStab in Algorithm 2. The number of groups P is a parameter of the method which can be fixed according to the number of sources and their configuration.

IV. Simulation Results

In this section, we study the convergence speed of the proposed method. The Partial-Block BiCGStab algorithm is compared to the BiCGStab and Block-BiCGStab algorithms for different numbers of sources and for highly contrasted dielectric objects. A setup configuration that can be found in the microwave tomography literature [2] is simulated. We consider $n_S = 96$ sources at frequency 2.45 GHz embedded in the air of permittivity $\epsilon_b = 1$. We note the wavelength in the background medium λ_b. The sources are split in three coaxial circles at heights $-\lambda_b$, 0 and λ_b, so that there are 32 sources equally distributed on each circle. The circle radius is $1.5\lambda_b$. A dielectric object is immersed in a cubic domain V with side λ_b. The setup is shown in Fig. 1. The domain V is discretized into $40 \times 40 \times 40$ voxels. With such a discretization, the n_S linear systems from (3) are of size $3 \times 40^3 = 192,000$. The object is composed of a cube with side $0.5\lambda_b$ and constant contrast equal to $\chi_1 = 3 - 1.5j$. Inside this lossy cube, a cuboid is inserted with square cross-section of side $0.25\lambda_b$ and the same height as the larger cube. The inner cuboid has contrast $\chi_2 = 4 - 3j$.

Algorithm 2 Block-BiCGStab algorithm

For an initial guess $\mathbf{E}_0$, $\mathbf{R}_0 = \mathbf{E}^{\text{inc}} - \mathbf{L}\mathbf{E}_0$, $\mathbf{P}_0 = \mathbf{R}_0$
Choose an arbitrary $\widetilde{\mathbf{R}}_0$ ($n \times n_S$ matrix)
$k = 0$
while $\left(\exists\, \boldsymbol{r}_{k_i}$ such that $\|\boldsymbol{r}_{k_i}\|/\|\boldsymbol{e}_i^{\text{inc}}\| > \text{tolerance}\right)$ where $\boldsymbol{r}_{k_i}$ is the i-th column of $\mathbf{R}_k$ **do**
  $\mathbf{V} = \mathbf{L}\mathbf{P}_k$
  solve $(\widetilde{\mathbf{R}}_0^\dagger \mathbf{V})\mathbf{A} = \widetilde{\mathbf{R}}_0^\dagger \mathbf{R}_k$
  $\mathbf{S} = \mathbf{R}_k - \mathbf{V}\mathbf{A}$
  $\mathbf{T} = \mathbf{L}\mathbf{S}$
  $\omega = \langle \mathbf{T}, \mathbf{S} \rangle_F / \langle \mathbf{T}, \mathbf{T} \rangle_F$
  $\mathbf{E}_{k+1} = \mathbf{E}_k + \mathbf{P}_k \mathbf{A} + \omega \mathbf{S}$
  $\mathbf{R}_{k+1} = \mathbf{S} - \omega \mathbf{T}$
  solve $(\widetilde{\mathbf{R}}_0^\dagger \mathbf{V})\mathbf{B} = -\widetilde{\mathbf{R}}_0^\dagger \mathbf{T}$
  $\mathbf{P}_{k+1} = \mathbf{R}_{k+1} + (\mathbf{P}_k - \omega \mathbf{V})\mathbf{B}$
  $k \leftarrow k + 1$
end while

Algorithm 3 Partial-Block BiCGStab algorithm

Build subsets $\mathbf{E}^{\text{inc}^p}$ for $p = 1 \dots P$ by partitioning the n_S sources.
for $p = 1 \dots P$ **do**
  Run the Block-BiCGStab algorithm on $\mathbf{E}^{\text{inc}^p}$ instead of $\mathbf{E}^{\text{inc}}$.
end for

Simulations were carried out using Matlab. The initial guesses of the total fields $\boldsymbol{e}_0$ and $\mathbf{E}_0$ were set to zero. Note that simulations with initializations at the incident fields $\boldsymbol{e}^{\text{inc}}$ and $\mathbf{E}^{\text{inc}}$ were also performed. The global behavior of the algorithms is similar for both initializations. The choice of the stopping criterion corresponds to a tradeoff between accuracy and computing time. The BiCGStab algorithm is usually stopped when the relative residual error $\|\boldsymbol{r}_k\|/\|\boldsymbol{e}^{\text{inc}}\|$ is small enough. For Block-BiCGStab and Partial-Block BiCGStab, the algorithm is stopped when all the relative residual errors are small enough, *i.e.,* for all i, $\|\boldsymbol{r}_{k_i}\|/\|\boldsymbol{e}_i{}^{\text{inc}}\| <$ tolerance, where $\boldsymbol{r}_{k_i}$ is the residual error of the i-th source at the iteration k, *i.e.,* the i-th column of $\mathbf{R}_k$. A tolerance of 10^{-3} on the relative residual errors is commonly accepted as a good tradeoff [1].

Fig. 2 presents the cost of BiCGStab and Block-BiCGStab as a function of the number of sources. The mean time per source for BiCGStab (solid line) is constant regardless of the number of sources, which is expected. For less than about 40 sources, the Block-BiCGStab method (dash-dot line) gives better performance than BiCGStab. However, it becomes less efficient than BiCGStab for larger numbers of sources: because of the ill-conditioning of matrix $\widetilde{\mathbf{R}}_0^\dagger \mathbf{V}$, more iterations are required. According to Fig. 2, groups of 20 to 40 sources correspond to the best performance of Block-BiCGStab. Subsequently, the group size for the Partial-

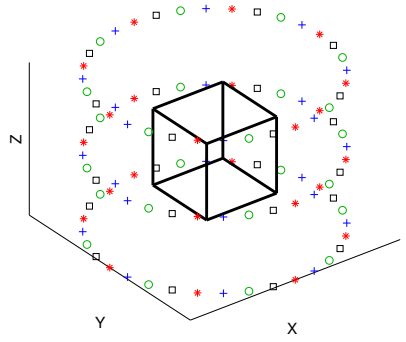

Fig. 1. Configuration setup with 96 sources distributed on three circles. The cube represents the discretized volume V. The four different symbols denote the four subgroups of sources used in the Partial-Block BiCGStab algorithm.

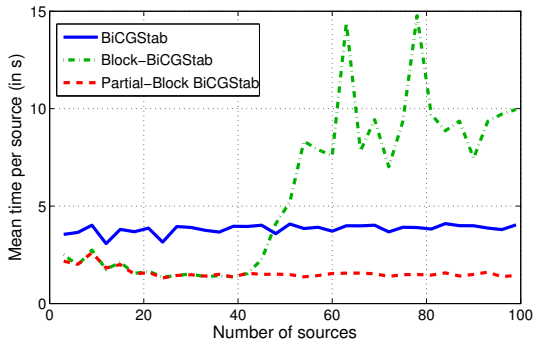

Fig. 2. Mean resolution time per source as a function of the number of sources for BiCGStab (full line), for Block-BiCGStab (dash-dot line) and for Partial-Block BiCGStab (dashed line)

Block BiCGStab algorithm is set to 24 sources. For our configuration with 96 sources, four groups of 24 sources are created. Fig. 1 illustrates the adopted partition where close sources do not belong to the same group, so as to reduce the linear dependence. Partial-Block BiCGStab is compared to BiCGStab and Block-BiCGStab in Fig. 2. When the number of sources is small, Partial-Block BiCGStab is as efficient as Block-BiCGStab and more efficient than BiCGStab. When the number of sources is large, the mean time per source remains constant and Partial-Block BiCGStab preserves the advantage over BiCGStab, thanks to the partition into groups.

Fig. 3 shows the 96 relative residual errors for BiCGStab, Block-BiCGStab and Partial-Block BiCGStab as functions of the iteration number. For BiCGStab, the tolerance is reached in between 22 and 40 iterations for a total time of 378 seconds. The Block-BiCGStab algorithm converges in 75 iterations (about 1000 seconds). The Partial-Block BiCGStab algorithm run on the four subgroups requires 10 or 11 iterations for a total time of 141 seconds. Such computing time values correspond to the results in Fig. 2 with 96 sources. The Partial-Block BiCGStab method converges faster and in a smoother way than the two other algorithms.

Table I presents the computational time and the total number of iterations for BiCGStab and Partial-Block BiCGStab and for different contrasts. The contrast factor α is defined as a multiplicative factor on the previous object. That is, for $\alpha = 1$, the object contrasts are $\chi_1 = 3 - 1.5j$ and $\chi_2 = 4 - 3j$. First we note that, for highly contrasted objects, the BiCGStab algorithm requires a large number of iterations to converge. For instance, for $\alpha = 1.5$, the BiCGStab algorithm converges in between 29 and 1888 iterations. Such a slow convergence results in a large computing time. Moreover, the symbol – in Table I means that some illuminations did not reach the tolerance after a large number of iterations (set to 5000). On the other hand, the Partial-Block BiCGStab method converges in much fewer iterations. For $\alpha = 1.5$, it converges in 14 or 15 iterations and the computational cost is 23 times lower than BiCGStab. For higher constrasts ($\alpha > 1.5$), the Partial-Block BiCGStab algorithm still reaches the required tolerance with a good speed of convergence.

Contrast factor α	0.5	1	1.5	2
BiCGStab				
Computing time (s.)	133	378	4567	–
Min number of iterations	10	22	29	53
Average number of iterations	10.7	31.7	384	–
Max number of iterations	11	40	1888	–
Partial-Block BiCGStab				
Computing time (s.)	101	141	196	217
Min number of iterations	7	10	14	17
Average number of iterations	7	10.75	14.75	17.25
Max number of iterations	7	11	15	18

TABLE I
COMPARISON OF BICGSTAB AND PARTIAL-BLOCK BICGSTAB FOR DIFFERENT CONTRASTS.

V. DISCUSSION AND CONCLUSION

In the context of 3-D iterative microwave image reconstruction, several forward problems must be solved repeatedly, each of which corresponding to a large scale linear system resolution. Such a computationally intensive task constitutes a bottleneck for realistic applications. In this paper, we proposed to speed up the resolution of the linear systems by drawing advantage from the fact that the linear matrix operator is common to all of them.

More precisely, we have explored the possibility to replace the usual BiCGStab algorithm by a block version. We have found that an optimal tradeoff was to divide the problem into several subproblems, each being separately solved by a Block BiCGStab algorithm. The proposed Partial-Block BiCGStab scheme is faster than both the standard and the Block BiCGStab versions. In more precise terms:

- For an object of moderate constrast, we have obtained a speedup factor between one and two with respect to BiCGStab. For an object of higher constrast, the acceleration can be larger than an order of magnitude. In such a case, slowdowns and even convergence failures are observed for BiCGStab, while the proposed Partial-Block BiCGStab version still produces a regular decrease of residual errors.
- The superiority of the Partial-Block version over the Block BiCGStab is related to the number of systems to

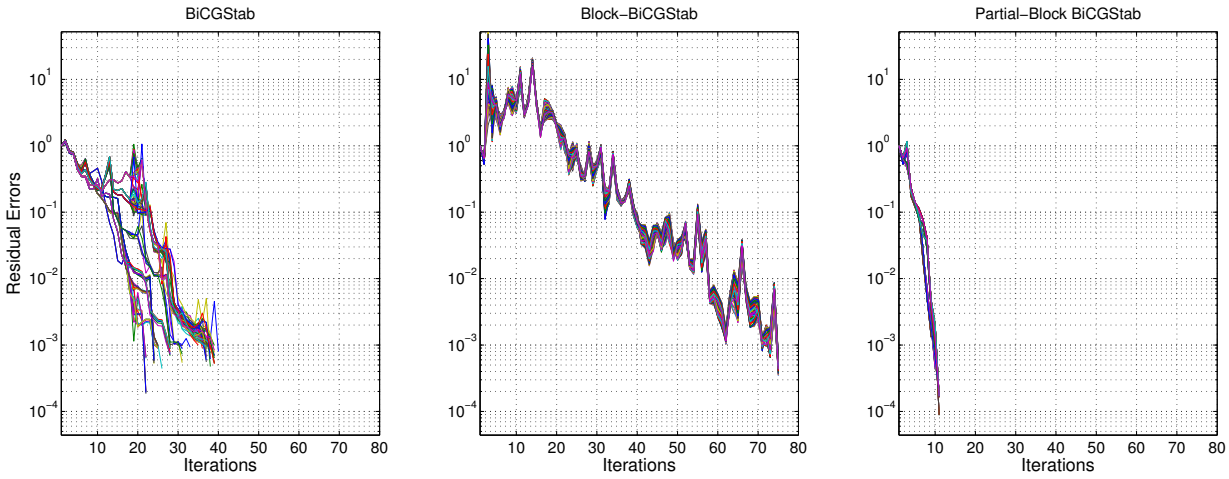

Fig. 3. Relative residual errors of the 96 forward problems as a function of iterations for BiCGStab, Block-BiCGStab and Partial-Block BiCGStab with $P = 4$ groups of 24 sources. The computing time corresponding to this simulation is respectively 378, 1004 and 141 seconds.

be solved and to the correlation between the right-hand side vectors. When many correlated vectors are jointly considered, Block BiCGStab becomes inefficient, because it relies on the explicit inversion of a matrix that becomes ill-conditioned. In the microwave imaging context, each right-hand side vector corresponds to an illumination, so we have proposed to spread close sources over distinct blocks along the Partial-Block BiCGStab strategy. In this way, a fast convergence has been obtained, without any instability.

Finally, the capacity of parallelization of the tested versions of BiCGStab remains to be discussed. On the one hand, the separate use of standard BiCGStab for solving each forward problem is easily parallelizable, as proposed in [2], [7]. On the other hand, the parallelization of Block BiCGStab is less straightforward and potentially less efficient, since it would correspond to a nested scheme where inner arithmetic operations would be distributed over different processors. Partial-Block BiCGStab inherits its capacity of parallelization from the two sides. On a multicore computer, a straightforward speedup factor can be obtained by spreading the Partial-Block BiCGStab runs over the available processors. On a massively parallel structure, the inner structure of each block should be also distributed. In the latter case, BiCGStab could appear as a better option than the proposed Partial-Block BiCGStab. However, we have empirically demonstrated that BiCGStab gradually becomes inefficient for objects of larger contrasts, while the numerical behavior of Partial-Block BiCGStab is more regular and efficient. The Partial-Block BiCGStab version may thus reach the best tradeoff in all situations, except for weakly contrasted objects and a massively parallel computing unit.

ACKNOWLEDGMENT

Partial support for this work was provided by NSERC Discovery Grant #138417-2012. The authors would like to thank Dr. Saïd Moussaoui for valuable discussions about the Block-BiCGStab algorithm.

REFERENCES

[1] Z. Q. Zhang, Q. H. Liu, C. Xiao, E. Ward, G. Ybarra, and W. T. Joines, "Microwave breast imaging: 3-D forward scattering simulation," *IEEE Trans. Biomed. Eng.*, vol. 50, no. 10, pp. 1180–1189, Oct. 2003.

[2] A. Abubakar, T. M. Habashy, G. Pan, and M.-K. Li, "Application of the multiplicative regularized Gauss-Newton algorithm for Three-Dimensional microwave imaging," *IEEE Trans. Ant. Propag.*, vol. 60, no. 5, pp. 2431–2441, May 2012.

[3] J. De Zaeytijd, A. Franchois, C. Eyraud, and J.-M. Geffrin, "Full-Wave Three-Dimensional microwave imaging with a regularized Gauss-Newton method; theory and experiment," *IEEE Trans. Ant. Propag.*, vol. 55, no. 11, pp. 3279–3292, Nov. 2007.

[4] P. Zwamborn and P. M. van den Berg, "The three dimensional weak form of the conjugate gradient FFT method for solving scattering problems," *IEEE Trans. Microwave Theory Tech.*, vol. 40, no. 9, pp. 1757–1766, Sep. 1992.

[5] Q. H. Liu, Z. Q. Zhang, T. T. Wang, J. Bryan, G. A. Ybarra, L. W. Nolte, and W. T. Joines, "Active microwave imaging. I. 2-D forward and inverse scattering methods," *IEEE Trans. Microwave Theory Tech.*, vol. 50, no. 1, pp. 123–133, 2002.

[6] H. A. Van der Vorst, "Bi-CGSTAB: A fast and smoothly converging variant of Bi-CG for the solution of nonsymmetric linear systems," *SIAM J. Stat. Sci. Comp.*, vol. 13, no. 2, pp. 631–644, 1992.

[7] A. Golnabi, P. Meaney, N. Epstein, and K. Paulsen, "Microwave imaging for breast cancer detection: Advances in three-dimensional image reconstruction," in *Proc. IEEE EMB Intern. Conf.*, Aug 2011, pp. 5730–5733.

[8] D. P. O'Leary, "The block conjugate gradient algorithm and related methods," *Linear Alg. Appl.*, vol. 29, pp. 293–322, 1980.

[9] Q. Fang, P. M. Meaney, S. D. Geimer, A. V. Streltsov, and K. D. Paulsen, "Microwave image reconstruction from 3-D fields coupled to 2-D parameter estimation," *IEEE Trans. Medical Imaging*, vol. 23, no. 4, pp. 475–484, Apr. 2004.

[10] A. El Guennouni, K. Jbilou, and H. Sadok, "A block version of BiCGSTAB for linear systems with multiple right-hand sides," *ETNA*, vol. 16, no. 129-142, p. 2, 2003.

[11] M. Pastorino, *Microwave imaging*. John Wiley & Sons, 2010, vol. 208.

[12] R. F. Harrington and J. L. Harrington, *Field computation by moment methods*. Oxford University Press, 1996.

[13] A. Abubakar and P. M. van den Berg, "Iterative forward and inverse algorithms based on domain integral equations for three-dimensional electric and magnetic objects," *J.Comput. Phys.*, vol. 195, no. 1, pp. 236–262, 20 Mar. 2004.